Optics Communications 407 (2018) 153–164

Contents lists available at ScienceDirect

Optics Communications

journal homepage: www.elsevier.com/locate/optcom

Power budget improvement of symmetric 40 Gb/s TWDM based PON2 system utilizing DMLs and DCF technique

Salem Bindhaiq [a,*], Nadiatulhuda Zulkifli [a], Abu Sahmah M. Supa'at [a], Sevia M. Idrus [a], M.S. Salleh [a,b]

[a] Innovative Engineering Research Alliance, Lightwave Communications Research Group, Photonics Simulation Laboratory, Universiti Technologi Malaysia, 81310 Johor, Malaysia

[b] Photonic Communication Technologies, Telecom Malaysia (TM), R&D Sdn Bhd, Cyberjaya 63000, Malaysia

ARTICLE INFO

Keywords:
Passive optical networks (PONs)
Next-generation passive optical network stage 2(NG-PON2)
Time and wavelength division multiplexing passive optical network (TWDM-PON)
Directly modulated lasers (DMLs)
Dispersion compensation fiber (DCF)
Power budget

ABSTRACT

In this paper, we propose to use optical dispersion compensation based on the widely deployed compensating fiber (DCF) employing directly modulated lasers (DMLs) to improve the power budget in a symmetric 40 Gb/s time and wavelength division multiplexed-passive optical network (TWDM-PON) systems. The DML output waveforms in terms of output optical power, bandwidth enhancement factor (α) characteristics are investigated in order to minimize the effect of DML chirp and improve the transmission performance. Simulation results show dispersion compensation of up to 140 km of SMF with power budget of 56.6 dB and less than 2 dB dispersion penalty. The feasibility of bandwidth enhancement factor and power budget is also investigated. The simulation results indicate sufficient dispersion compensation for TWDM-PON based on DML transmission, which may vary considerably in their practical demonstration due to different system characterization.

1. Introduction

The incessant rise of bandwidth demand in broadband access networks in both industry and academia is a challenge that requires intensive innovations to be satisfactorily met [1]. For instance, multimedia applications such as video on demand (3D video and super HD), cloud computing, social network, peer to peer file sharing and online gaming are main bandwidth drivers in future broadband convergence services [2]. Recently, time and wavelength division multiplexing-passive optical networks (TWDM-PON) have been a pragmatic solution in both industry and academia aspects for next generation-passive optical network second stage (NG-PON2) by full service access network (FSAN) group of telecom company members [3]. While the key technologies of TWDM-PON components are more likely as used in previous standardized PON systems, it could be of interest for researchers as well as the practitioners to take into serious consideration the application of these distinct technologies [4]. Such new applications will drive and utilize innovations to solve a near future problem in TWDM-PON architecture transmission, as the key issue for cost reduction in TWDM-PON investment can be realized by improving the power budget. Thus, there is a great demand for high power budget transmission in TWDM-PON deployment. Direct modulated lasers (DMLs) have the potential to satisfy the key TWDM-PON technologies, such as optical network unit (ONU) transmitters due to its benefits such as lower cost implementation, compactness, small power consumption, and high optical output power transmitter [5,6]. However, the major technical challenges associated with the use of DML are wavelength frequency chirp that limits the modulation bandwidth of the DML and the dispersion-induced waveform distortions [7–11]. To apply DML to 10 Gb/s transmission systems and further to 40 Gb/s TWDM-PON application to combat the limited modulation bandwidth of our laser sources as well as chromatic dispersion for higher power budget, a detailed knowledge of DML chirp and allowable dispersion is required. Table 1 summarizes transmission results from the literature which use TWDM-PON DMLs for power budgets improvement and have set a record in terms of modulation format, method utilized, distance, splitting ratio and achievable power budget. It provides the readers with an overview on the current state of the art in terms of TWDM-PON based DML capabilities for the purpose of the power budget improvement.

Several interested research groups have been actively targeting DML-based 40 Gb/s TWDM-PON for power budget improvement, as summarized in Table 1, where the results of power budget are listed based on the achievable value, which is the aim of this paper. An alternative

* Correspondence to: Innovative Engineering Research Alliance, Universiti Technologi Malaysia (UTM), Johor 81310, Malaysia.
E-mail address: Salembindhaiq05@gmail.com (S. Bindhaiq).

http://dx.doi.org/10.1016/j.optcom.2017.09.027
Received 15 March 2017; Received in revised form 6 September 2017; Accepted 7 September 2017
Available online 21 September 2017
0030-4018/

Table 1
Recent development on 40 Gb/s TWDM-PON utilizing DML for power budget improvement.

Ref	ModulationFormat	Method utilized	Distance (km)	Splittingratio	Power budget (dB)
[12]	NRZ	TOF	25	256	31
[13]	Duo-binary	DI	40	64	31
[14]	NRZ- (OEQ)	DI	40	NA	36
[15]	NRZ	NA	20	512	37
[16]	NRZ	DI	50	256	38
[17]	NRZ	TOF	25	1000	39
[5]	NRZ	DI	100	64	43.2
[18]	NRZ	SOA	40	2000	51
[19]	NRZ	DI	100	512	53

way to improve the power budget is reported by *Zhengxuan Li et al.* that utilize the advantages of the ability of a tunable optical filter (TOF) to select the downstream signal, thereby helping to manage the DML upstream signal chirp. This enables the TWDM-PON system to support a reach of 25 km and 256 splitting ratio [12]. In [12], we find the 31 dB power budget is achieved where the NRZ modulation format is applied. A similar power budget of 31 dB is achieved in [13] by *Zhengxuan Li et al.* The purpose of the work is to improve the capacity of TWDM-PON DML with duobinary modulation format where delay interferometer (DI) is employed to mitigate the chromatic dispersion induced signal distortion where the system is capable of supporting 64 users within 40 km reach. *Zhengxuan Li et al.* extend the power budget of TWDM-PON system to 36 dB using DI to work as a dispersion compensator and an optical frequency equalizer (OEQ) [14]. This system uses NRZ-OEQ modulation that covers a reach of 40 km SMF. A power budget of 37 dB for TWDM-PON was achieved by *Yuanqiu Luo et al.* in [15] using DML with NRZ modulation format as the upstream laser source with a reach of 20 km. *Meihua Bi et al.* propose a TWDM-PON system with a DI at ONU to simultaneously realize the downstream differential phase shift keying (DPSK) signal demodulation and managed the upstream DML signal chirp for the first time with 38 dB power budget supporting 256 users along with 50 km SMF transmission [16]. Following that, *Lilin Yi et al.* present an improved TWDM-PON system to support a distance of 25 km with 39 dB power budget by changing the location of chirp management filter from ONU to optical line terminal (OLT) right after the preamplifier for upstream signals [17]. *Meihua Bi et al.* improve the power budget of a TWDM-PON system with DML using a DI at OLT for both downstream and upstream directions to extend the power budget of 43.2 dB over 100 km distance reach for a 64 split supportive system [5]. *Zhengxuan Li et al.* push the TWDM-PON system power budget using a semiconductor optical amplifier (SOA) to 51 dB power budget supporting 2000 users with 40 km passive reach [18]. *Zhengxuan Li et al.* . improve the TWDM-PON system power budget through DI along with optical amplifier, such as Raman amplifier and erbium doped fiber amplifiers (EDFAs), to 53 dB power budget supporting 512 users with 100 km passive reach [19]. It is worth noting that all of the results at 53 dB of power budget for 40 Gb/s TWDM-PON system have been obtained with an essentially NRZ DML transmission system. It is also noted that the 40 Gb/s TWDM-PON system based DML transmission still have capability to support higher power budget record for further service to remote places.

In this paper, we propose to use a DCF in OLT employed 10 Gb/s NRZ DMLs to improve the power budget of symmetric 40 Gb/s TWDM-PON system. Initially, the dynamic behavior of 10 Gb/s NRZ DML is analyzed using a theoretical approach of DML output characterization such as the output power (bias current), bandwidth enhancement factor (α) characteristics in order to predict the lowest DML chirp required to enhance the spectral width of the DML, is presented. The simulation results show a power budget of 56.6 dB after transmission over 140 km SMF and 512 users for 40 Gb/s TWDM-PON system. Our simulation results demonstrate a sufficient dispersion compensation for DML-based TWDM-PON transmission system. While results are not absolute due to variations that can occur in practical implementation, our analysis demonstrates the feasibility of using DCF to improve the power budget of 40 Gb/s TWDM-PON links.

The paper is organized as follows. The transmission performance of 10 Gb/s DML with dispersion compensation is described in Section 2. This includes DML theoretical approach and 10 Gb/s DML transmission performance. The symmetric 40 Gb/s TWDM-PON with dispersion compensation is presented in Section 3. Section 4 investigates the feasibility of the bandwidth enhancement factor and dispersion compensation with power budget. Finally, conclusion is given in Section 5.

2. Transmission performance of 10 Gb/s DML with dispersion compensation

2.1. DML theoretical approach

Let us make the optical source of DML centered at $\omega_o = 2\pi\nu_o$ which is modulated by both intensity and phase components. Hence, the complex optical field at the output of the light source is given by [20]:

$$E_{in}(t) = \sqrt{I_{in}(t)}\exp\left(j\Phi_{in}(t)\right)\exp\left(j\omega_o t\right) \tag{1}$$

where $I_{in}(t)$ represents the intensity modulation signal that can be expressed as:

$$I_{in}(t) = P_{in}(t) = P_o\left(1 + m_{IM}\cos\left(\omega t + \varphi_{IM}\right)\right) \tag{2}$$

where P_o is the output power, m_{IM} is the intensity modulation index, ω is the angular modulation frequency and φ_{IM} is the phase associated with the intensity modulation term. The direct current term stands for the necessary bias and the amplitude of the signal is proportional to $\sqrt{P_{in}(t)}$. The relation between amplitude and intensity modulations can be written in the form:

$$\sqrt{P_{in}(t)} \cong \sqrt{P_o}\left(1 + \frac{m_{IM}}{2}\cos(\omega t)\right) = A_o\left(1 + m_{AM}\cos(\omega t)\right) \tag{3}$$

where A_o is the mean amplitude of the signal and m_{AM} represents amplitude modulation index. The phase modulation $\Phi_{in}(t)$ can be written in the form:

$$\Phi_{in}(t) = m_{PM}\cos\left(\omega t + \varphi_{PM}\right) \tag{4}$$

where m_{PM} is the phase modulation index and φ_{PM} is the initial phase associated to $\Phi_{in}(t)$. For simplicity, we can note Eq. (1) can be a function of the phase difference as $\Delta\varphi = \varphi_{PM} - \varphi_{IM}$, so then:

$$P_{in}(t) = P_o\left(1 + m_{IM}\cos(\omega t)\right) \tag{5}$$

$$\Phi_{in}(t) = m_{PM}\cos\left(\omega t + \varphi_{PM}\right). \tag{6}$$

Hence, the phase $\Phi_{in}(t)$ in Eq. (1) depends on the modulation of the optical frequency of the light source caused by $I_{in}(t)$. Indeed, the chirp of the light source that arrives due to the changing of its polarization current during the intensity modulation will cause a variation in the carriers' density and this will directly affect the source's refractive index. The phase modulation contribution is coupled to intensity modulation, meaning that $\Phi_{in}(t)$ is a function of P_{in}.

2.1.1. Rate equation model

The signal single mode rate equations are a set of coupled ordinary differential equations that described relationship between carrier density N and photon density S [21].

$$\frac{dS(t)}{dt} = \Gamma g_o \left(N(t) - N_o\right) \frac{S(t)}{(1+\varepsilon)} - \frac{S(t)}{\tau_p} + \frac{\Gamma \beta_{sp}}{\tau_e} N(t) \tag{7}$$

$$\frac{dN(t)}{dt} = \frac{I(t)}{qV} - \frac{N(t)}{\tau_e} - g_o \left(N(t) - N_o\right) \frac{S(t)}{(1+\varepsilon S(t))} \tag{8}$$

$$R_{sp} = AN(t) + BN(t)^2 + CN(t)^3 \tag{9}$$

where Γ is the confinement factor, N_o is the carrier density at transparency, τ_p and τ_e are the photon and electron lifetimes, respectively, β_{sp} is the fraction of spontaneous emission coupled into the lasing mode, q is the electron charge, V is the active layer volume, ε is the gain compression, g_o is the gain slope constant, R_{sp} is carrier recombination rate, A is the non-radiative recombination rate, B is the radiative recombination coefficient and C is the Auger recombination coefficient. The gain slope constant can be expressed by $g_o = v_g a_o$, where v_g is the group velocity and a_o is the active layer gain coefficient.

2.1.2. DML chirp

The interaction between phase and intensity modulation in DML is described with the help of the laser rate equations, which describe how the changes in the carriers' density will influence the optical field inside the DML cavity. The relation between the instantaneous frequency and the optical modulation power is shown to be [22]:

$$\nu(t) = \nu_o + \Delta\nu(t) \tag{10}$$

$$= \frac{\alpha}{4\pi} \left(\kappa P(t) + \frac{1}{P(t)} \frac{dP(t)}{dt}\right) \tag{11}$$

$$\Delta\nu(t) = \frac{1}{2\pi} \frac{d\Phi(t)}{dt} \tag{12}$$

where α is the bandwidth enhancement factor. The DML chirp frequency $\nu(t)$ can be described as [22,23]. Eq. (11) shows the frequency chirp of DML is combination of adiabatic (Frequency modulation) and transient chirp (phase modulation) contributions. κ is adiabatic chirp coefficient which makes the transient chirp masked.

2.1.3. DML amplitude frequency response and bandwidth

When the DML is biased above threshold with a bias current I_b, and the signal modulation current I_m is added to the bias current, the total injection current can be described as [24]:

$$I = I_b + I_m. \tag{13}$$

As a result, when the bias current, above the threshold, we assume $I_b \gg I_m$ for small-signal modulation. It should be noted that the bandwidth of the DML would be enhanced based on the rate $\left(I_b - I_{th}\right)^{0.5}$ from the DML bandwidth Eq. (14) as:

$$\Delta B_{3-dBDML} \approx \left(\frac{3G}{4\pi^2 q}\left(I_b - I_{th}\right)\right)^{0.5} \tag{14}$$

where G is the damping rate ratio of the gain, q is electron charge. The relaxation oscillation frequency (f_r) can be approximately expressed by:

$$f_r \approx \left(\frac{G}{4\pi^2 q}\left(I_b - I_{th}\right)\right)^{0.5}. \tag{15}$$

The amplitude frequency response of the DML transmitter under small signal modulation can be expressed as [25]:

$$H_\omega(\omega) = \frac{\omega_r^2}{\omega_r^2 - \omega^2 + 2jG\omega} \tag{16}$$

where ω_r is the angular frequency of relaxation oscillation frequency $\omega_r = 2\pi f_r$.

2.1.4. DML Frequency response after SMF

In the chirped DML, the complex small signal transfer can be taken the expression form [25]:

$$H_{IM\leftrightarrow PM}(\omega) = \frac{2m_{PM}}{m_{IM}} \exp(j\Delta\varphi) = a + jb(\omega). \tag{17}$$

The part a represents a phase modulation (PM) component that will change both the dips' positioning and the lobes' height and $b(\omega)$ represents a frequency modulation (FM) component that has effect on depth of the dips of the channel. The frequency response of a dispersive intensity modulation/direct detection (IM)/(DD) channel can be written as [20]:

$$H_{IM/DD}(\omega) = \left|\cos(\theta) - \sin(\theta) H_{IM\leftrightarrow PM}(\omega)\right| \tag{18}$$

$$\theta = \frac{D\lambda^2\omega^2 z}{4\pi c} \tag{19}$$

where θ is related to the phase variation induced by the chromatic dispersion. D is the fiber dispersion parameter, λ is the wavelength of the optical signal, z is the transmission distance, and c is the speed of light in vacuum. It is possible to find the DML small-signal frequency response characterizing the chirp effect [20]:

$$H_{IM\leftrightarrow PM}(\omega) = \alpha - j\frac{\alpha\omega_c}{\omega} \tag{20}$$

$$\Delta\varphi = \tan^{-1}\left(-\frac{\omega_c}{\omega}\right) \tag{21}$$

$$\frac{2m_{PM}}{m_{IM}} = \sqrt{\alpha^2 + \left(\frac{\alpha\omega_c}{\omega}\right)^2} \tag{22}$$

$$\omega_c = \kappa p. \tag{23}$$

The frequency response of the dispersive SMF in DML/DD can be expressed as [20]

$$H_{IM/DD}(\omega) = \left|\cos(\theta) - \sin(\theta)\left(\alpha - j\frac{\alpha\omega_c}{\omega}\right)\right|. \tag{24}$$

When the DML chirp is mostly influenced by the pure PM term (transient chirp), Eq. (24) will be:

$$H_{IM/DD}(\omega) = \sqrt{1+\alpha^2}\cos\left(\theta + \tan^{-1}(\alpha)\right). \tag{25}$$

When the DML chirp is mostly influenced by the pure FM term (adiabatic chirp), Eq. (24) will be:

$$H_{IM/DD}(\omega) = \frac{\alpha\kappa p}{\omega}\sin(\theta). \tag{26}$$

Then, the total frequency response of the dispersive SMF in DML/DD can be expressed as [9]:

$$H_{IM/DD}(\omega) = \sqrt{1+\alpha^2}\cos\left(\theta + \tan^{-1}(\alpha)\right) + \frac{\alpha\kappa p}{\omega}\sin(\theta) \tag{27}$$

where P is the output power of the laser, and ω is the angular frequency of the modulated signal. The first and second terms of Eq. (27) approximately represent the transient and adiabatic chirp of DML, respectively.

2.2. Method

The optical link considered for symmetric 10 Gb/s directed modulated laser (DML) transmission is depicted in Fig. 1(a). For both downstream and upstream links, the DML employs a non-return-to-zero (NRZ) on–off-keying (OOK) modulation format and driven by 10 Gb/s pseudorandom binary sequence (length $= 2^{11} - 1$) where the confidence interval is 0.84 for 11 bits in data stream [26]. To practically generate the DML current, due to some limitation in our facilities, we assume that the bias current of 75 mA is set and applied to a DML with a multi-quantum well active layer operating at 1597.74 and 1544.11 nm for downstream and upstream direction, respectively, and exhibiting a threshold current of 10 mA which is set in the simulation. This assumption of bias current is inherited to meet practical agreement with the linewidth enhancement factor which is set to 2 in this work. The modulated optical signal generated at the output of the DML is

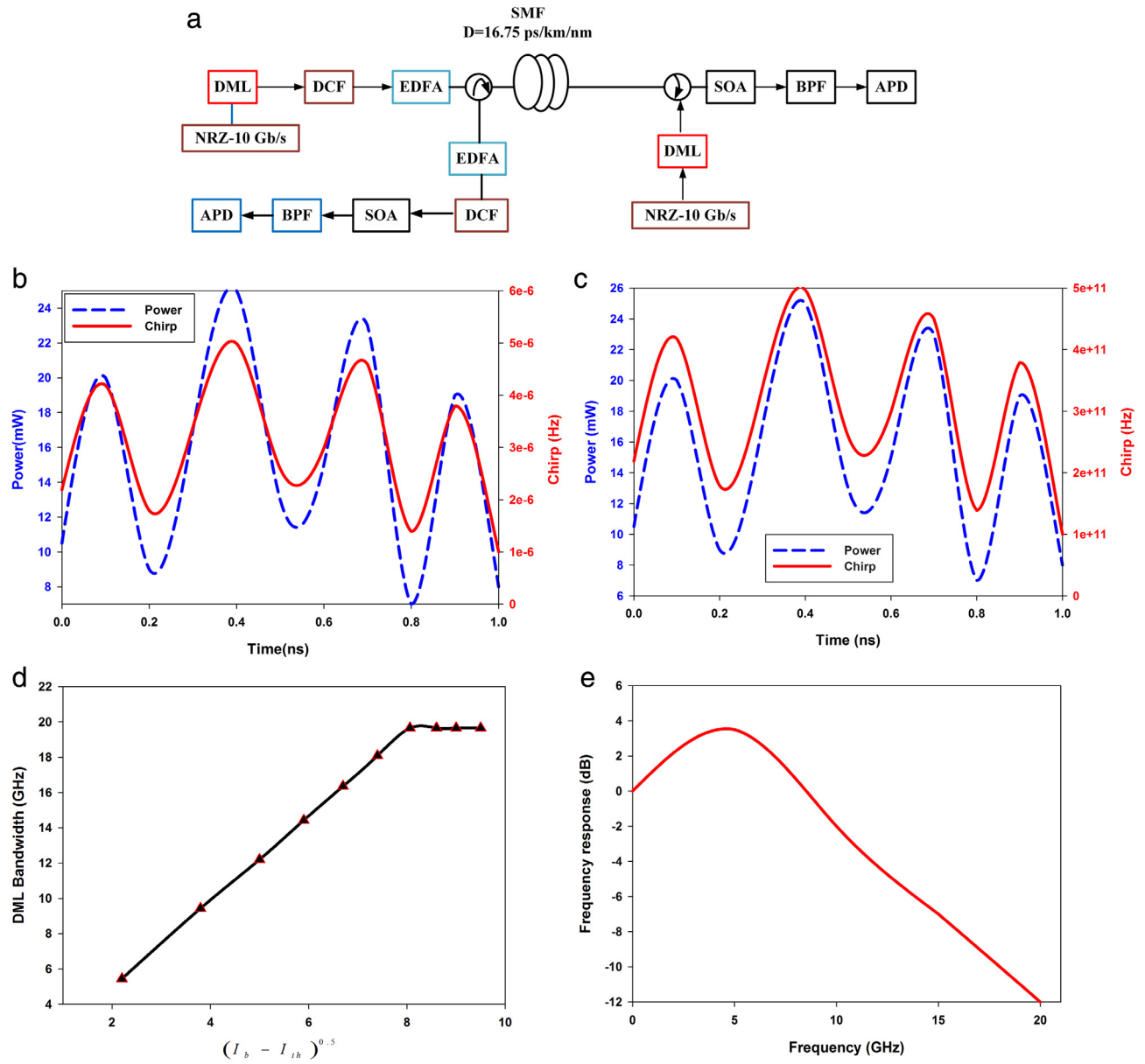

Fig. 1. (a) Symmetric 10 Gb/s DML with dispersion compensation. (b) Output optical power and chirp with $\kappa = 125 \times 10^{-5}$ Hz/w from Eq. (12). (c) Output optical power and chirp with $\kappa = 125 \times 10^{12}$ Hz/w from Eq. (12) (d) Relaxation oscillation frequency of the DML versus the square root of the bias current above threshold. (e) Frequency responses of the DML from Eq. (16).

transmitted over a dispersion compensator (DCF) with 13 km length to increase the chromatic dispersion transmission limit before being amplified by erbium-doped fiber amplifier (EDFA) and transmitted over a 140 km single mode fiber (SMF) with a dispersion parameter D = 16.75 ps/km/nm. A semiconductor optical amplifier (SOA) is used with gain of 18 dB and 7.5 dB noise figure (NF) to compensate for the loss. Note that the SOA can be replaced by a RSOA for cost effective purposes. However, in terms of good performance, SOA is preferred. A band pass filter (BPF) is then employed to filter out the effect of the amplified spontaneous emission (ASE) noise from the SOA. Then, the signal is detected by an avalanche photodiode (APD) at the receiver side. As for upstream link, the modulated optical signal generated at the output of the DML is transmitted over a single mode fiber (SMF) with a dispersion parameter D = 16.75 ps/km/nm. The upstream link is amplified by EDFA before a DCF is employed to enhance the transmission distance of 140 km SMF. Then, a SOA is used to improve the receiver sensitivity followed with a BPF to mitigate the effect of ASE, and the signal is then detected by an ADP receiver.

Typical values for the DML rate equation parameters can be found in Table 2 and are adequate for general simulation purposes. However, detailed knowledge of the rate equation parameters for a particular device is necessary to obtain close agreement between simulation and numerical results.

2.3. Numerical results

The power and chirp waveforms are shown in Fig. 1 (b and c) for different adiabatic chirp coefficient values. When using a DML transmitter with ($\kappa = 125 \times 10^{-5} Hz/w$) as shown in Fig. 1(b), a strongly dominated transits chirp behavior presents. The adiabatic chirp component is significantly lower than the transient chirp component. The time variations of the chirp do not strongly follow the optical power. This is because lasers with strongly dominated transient chirp behavior do not have a direct relationship between laser output power and generated chirp. When ($\kappa = 125 \times 10^{12} Hz/w$) as shown in Fig. 1(c), this exhibits a strongly adiabatic dominant chirp behavior. As the optical

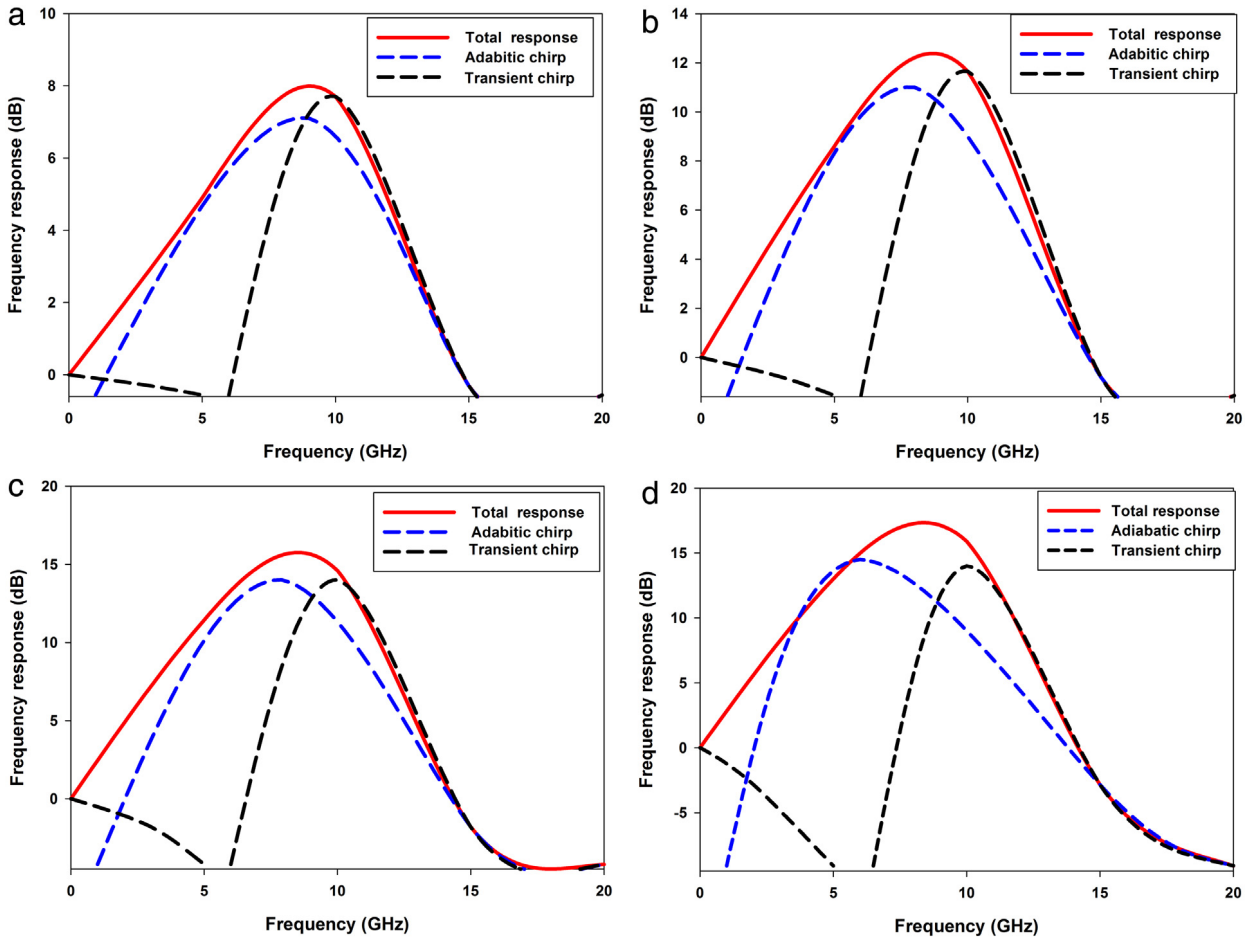

Fig. 2. Frequency response of the SMF induced by adiabatic and transient chirp after (a) 20 km, (b) 50 km, (c) 100 km, and (d) 140 km long transmission from Eq. (27).

power is proportional to the bias current, the time variations of the adiabatic chirp strongly follow the optical power. This is also due to the fact that the lasers with strongly dominated adiabatic chirp behavior have a direct relationship between laser output power and generated chirp. Despite the fact that with great bias current values and high optical power the adiabatic chirp is dominant over the transient chirp, the effects of whether adiabatic or transient chirp dominant in DMLs behavior is serious in terms of degrading the transmission performance for 10 Gb/s data rate unless real bandwidth enhancement factor is reduced.

Fig. 1(d) shows the relaxation oscillation frequency of the DML versus the square root of the bias current above threshold $\left(I_b - I_{th}\right)^{0.5}$. The DML used in this work exhibits a broad 3-dB bandwidth of 6 GHz when biased current is assumed to be at 75 mA, which equivalent to $\alpha = 2$. This bandwidth can be enhanced not only based on the bias current, but also the damping rate can help to enhance the DML bandwidth as shown in Eq. (14). While the physical origin of those oscillations is the interplay between the injected carriers and emitted photons, the oscillation frequency depends on the DML output power, hence on the value of the driving current as shown in Eq. (15). A high output power from DML can lead to help optical access networks in terms of securing a large power budget. This would lead to reduce the effect of waveform distortions caused by the relaxation oscillation of the laser diode when we increase the bias current. This is because the relaxation oscillation frequency of DML increases with $\left(I_b - I_{th}\right)^{0.5}$, where I_b is the bias current and I_{th} is the threshold current. The oscillation frequency increases with the bias current at a rate of 1.6 GHz/mA $^{1/2}$. As a result, the 3-dB bandwidth of the DML is enhanced to more than 7 GHz to accommodate 10 Gb/s DML, as shown in Fig. 1(e). The frequency response of DML also shows that we have a relatively flat response up to 5 GHz.

Fig. 2 shows that the adiabatic chirp serves to compensate for the frequency notch induced by the transient chirp because the notch caused by transient and adiabatic chirp, to some extent, appears at different frequencies until the frequency of 20 GHz as shown in Fig. 2. While the range of frequency corresponding to frequency response in this investigation is limited to 20 GHz and not compensated by adiabatic chirp, the bandwidth of the dispersive SMF in DML/DD, after the transmission over 140 SMF, is determined mostly by the notch frequency of the adiabatic chirp that can be written in referring to the notch frequency as:

$$Bw \approx \sqrt{\frac{c}{D\lambda^2 z}}. \tag{28}$$

We note that the bandwidth of DML after SMF transmission of 140 km does not depend on the DML's chirp parameters. The 3-dB bandwidth of the 140 km long SMF in a DML/DD system is 7.2 GHz obtained by using Eq. (27) which is met with the 3-dB bandwidth of the 140 km long SMF obtained by Eq. (28). The results show that when the adiabatic chirp parameter κ is very high, the transient chirp is compensated by the adiabatic chirp and both 3-dB bandwidth from Eqs. (27) and (28)) are in agreement. However, when the adiabatic chirp parameter κ is very small, the transient chirp cannot be compensated by the adiabatic chirp and, in this case, the bandwidth of the optical fiber is limited by the frequency notch induced by the first transient chirp. In any case, while the bandwidth enhancement factor α of a DML typically is 2, we conclude that the bandwidth of SMF in a DML/DD system is mainly determined by the accumulated chromatic dispersion rather than the laser's chirp parameters.

Table 2
System simulation parameters.

DML		
Parameter	Symbol	Value
Active-region volume	V	$3 \times 10^{-13} cm^3$
Confinement factor	Γ	0.229
Gain compression factor	ϵ	$0.259 \times 10^{-17} cm^3$
Linewidth enhancement factor	α	2
Differential quantum efficiency	γ_o	0.19
Photon lifetime	τ_p	$770ps$
Electron lifetime	τ_e	$1.6ps$
Spontaneous emission factor	β_{sp}	1.8×10^{12}
Carrier density at transparency	N_o	$1.23 \times 10^{18} cm^{-3}$
Group velocity	v_g	$8 \times 10^9 cm/s$
Gain constant	a_0	$9.5 \times 10^{-16} cm^2$
Damping rate	G	3
DCF		
Parameter	Value	
Dispersion at reference of 1550 nm	$-80ps/nm/km$	
Length	13 km	
Attenuation	$0.5dB/km$	
Dispersion Slope	$0.07ps/nm^2/km$	
SMF		
Parameter	Value	
Dispersion at reference of 1550 nm	$16.75ps/nm/km$	
Length	140 km	
Attenuation	$0.2dB/km$	
Dispersion Slope	$0.075ps/nm^2/km$	
APD		
Parameter	Value	
Responsivity	$1A/W$	
Thermal noise	$1.84 \times 10^{-22} W/Hz$	

2.4. Comparison simulation results with theoretical results

Fig. 3 shows a comparison of the simulated frequency response using optical communication system design software and theoretical frequency response using Eq. (16) with the function of frequency revealing a close agreement as shown in Fig. 3(a). Both the calculated and simulated responses showed a broad peak at around 5 GHz. However, the simulated response has some fluctuation due to the simulation environment relaxation oscillation while the theoretical is obtained by constant values. Despite this argument, the trend is clear and our model provides good approximations. Overall, this most likely reflects the accuracy of the simulation and the theoretical parameters and trends. That said, it is important to note that the simulation results are not really exact for TWDM-PON and DML characterization performance when compared to practical demonstration.

We compare the theoretical chirp waveforms with the simulated results as shown in Fig. 3(b). The calculations are using Eq. (12). We obtained a good agreement between the calculated and the measured waveforms. The calculated chirp is 4.5×10^{11} Hz for peak to peak waveform. This is close to the simulated value of about 4.45×10^{11} Hz as shown in Fig. 3(b). This certainly reflects the accuracy of the simulated and the calculation parameters. It can be seen that both simulated and calculated chirp of some peaks have likely view of overshot at different samples of certain times due to the different environments in terms of relaxation oscillation frequency. However, the obtained simulation waveform and calculated waveforms with the signal rate equation waveform model have shown close agreements and as well as reasonable prediction.

Fig. 4 illustrates a comparison between simulation and theoretical results after SMF distance transmission. The results show that the simulated frequency responses agree with the theoretically calculated values obtained by using Eq. (27). However, it can be noted from Fig. 4 that some differences appear at frequency of 12 GHz between the theoretical and simulated curves due to the start of dip frequency

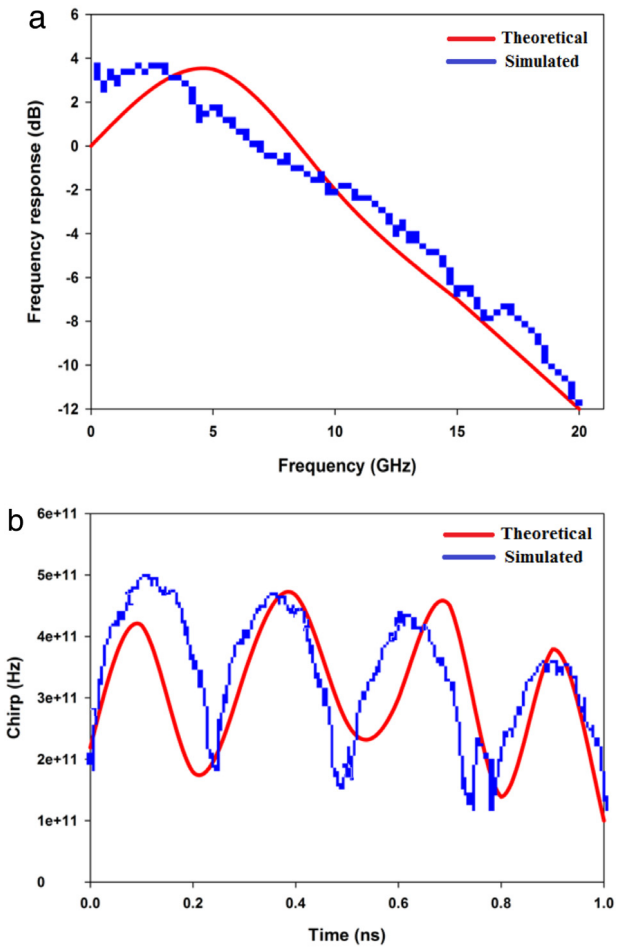

Fig. 3. Comparison of theoretical and simulated results for (a) frequency response and (b) waveform chirp.

induced by the transient chirp of DML effect. Fig. 4 investigates the theoretical frequency response as a function of frequency in an attempt to study the impact of the adiabatic and transient chirp of DML after SMF 140 km.

2.5. Transmission performance

We evaluate the back-to-back (BTB) performance of the single channel performance of both downstream and upstream transmissions and compare with the results from 140 km bidirectional SMF transmissions as shown in Fig. 5. As an illustration, we showed the BERs and sensitivities at 1597.74 nm and 1544.11 nm in the downstream and upstream directions, respectively. At a BER of 10^{-5}, the power penalty after 140 km with SOA and DCF transmission, and with SOA and without DCF transmission for the downstream direction is 10.5 dB, while it has been observed at 10 dB for the upstream direction as shown in Fig. 5(a) and (b), respectively.

The receiver sensitivity with SOA and DCF transmission is about -38.1 dBm while with SOA and without DCF transmission is -27.6 dBm for the downstream direction. For the upstream direction, the obtained receiver sensitivity with SOA and DCF transmission is -38.5 dBm while it is about -28.5 dBm when SOA is used and without DCF transmission. For the case of BTB transmission, at a BER of 10^{-5}, the power penalty for BTB with SOA and DCF transmission, and BTB with SOA and without DCF transmission is 3.6 and 5.1 dB for downstream and upstream directions respectively. The receiver sensitivity in terms of SOA and DCF transmission is -22.9 dBm while with SOA and without

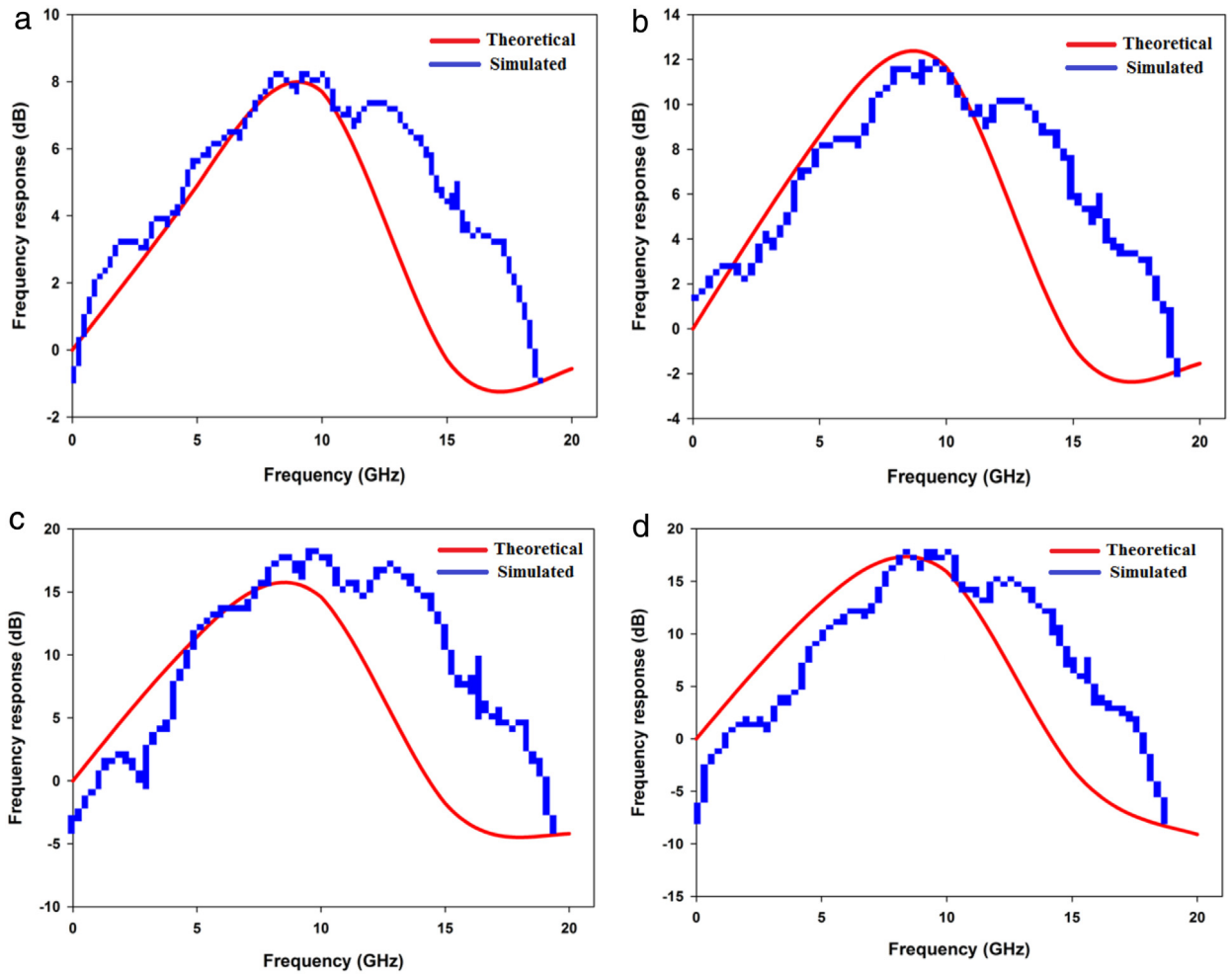

Fig. 4. The simulated frequency responses of SMF in a DML system in comparison with the theoretically calculated curves by using Eq. (27).

DCF transmission is -19.3 dBm for downstream direction. For the upstream direction, the obtained receiver sensitivity with SOA and DCF transmission is -24.4 dBm while it is obtained at -19.3 dBm when SOA is used without DCF transmission. The power penalties are mainly caused by the filtering effects at the ONU and OLT, and the accumulated fiber dispersion during the transmissions. The wavelength band utilized in both downstream and upstream directions can also lead to dispersion penalties due to the condition of the wavelengths in that band. Note that the receiver sensitivity for the downstream and upstream signals after 140 km is better than the BTB transmission because the right control of SOA's injection power plays a significant role to improve the receiver sensitivity.

Next, the eye diagrams and the sensitivities of the signal in both directions at transmission distances of 0, 30, 60, 100 and 140 km are performed, and the results are shown in Fig. 6. For both directions, the evaluation was carried out using DML with a launched power of 20 dBm and operating wavelength of 1597.74 nm and 1544.11 nm for downstream and upstream directions, respectively. At 0 km or BTB, both downstream and upstream directions show good performance. Upon transmission distance increment to 30 km, a degradation of eye diagram quality can be observed for both directions. For the 60 km case, the eye diagram is distorted gradually for both downstream and upstream sides, as illustrated in Fig. 6 (a) and (b). With increasing fiber transmission distance to 100 and 140 km for both sides, the qualities are worse than the previous cases. This is caused by the higher accumulated residual chromatic dispersion at increased transmission distances. The findings show that the negative dispersion effect from DCF can effectively compensate for the positive dispersion from SMF. It should be noted that until 140 km, the eye diagram is still not completely closed which is possible with the assistance of the proposed scheme.

3. 40 Gb/s TWDM-PON with dispersion compensation

3.1. Method

Fig. 7 shows the system architecture of a symmetric 40 Gb/s TWDM-PON that utilizes the proposed DCF where 10 Gb/s four pair wavelengths are stacked to achieve 40 Gb/s aggregate data transmission for both upstream and downstream links. The key feature of the proposed DCF scheme is to extend transmission distance since it has an adverse dispersion effect. Therefore, it is preferred for long PON applications. In each transmitter (TX) block of the OLT, a low cost DML is driven by 10 Gb/s PRBS with a word length of $2^{11} - 1$. In this demonstration, we utilize a short PRBS length of $2^{11} - 1$ to minimize the pattern effects. Then, the signals are multiplexed by a WDM MUX and injected into a DCF. After the WDM MUX and DCF, the signals are amplified by an erbium-doped fiber amplifier (EDFA) with 23 dB gain and 3.5 dB noise figure (NF). Passing through the 140 km SMF, the signals are distributed to each ONU by a splitter at the RN. At the ONU side, an SOA amplifies all the four downstream channels with 18 dB gain and 6 dB NF to compensate for the losses. Then, a tunable optical filter (TOF) is employed to select the desired channel and suppresses the ASE noise from SOA before the signal is launched into the APD detector at the receiver (RX). The downstream wavelengths are set at 1596.14, 1596.94, 1597.74 and 1598.54 nm.

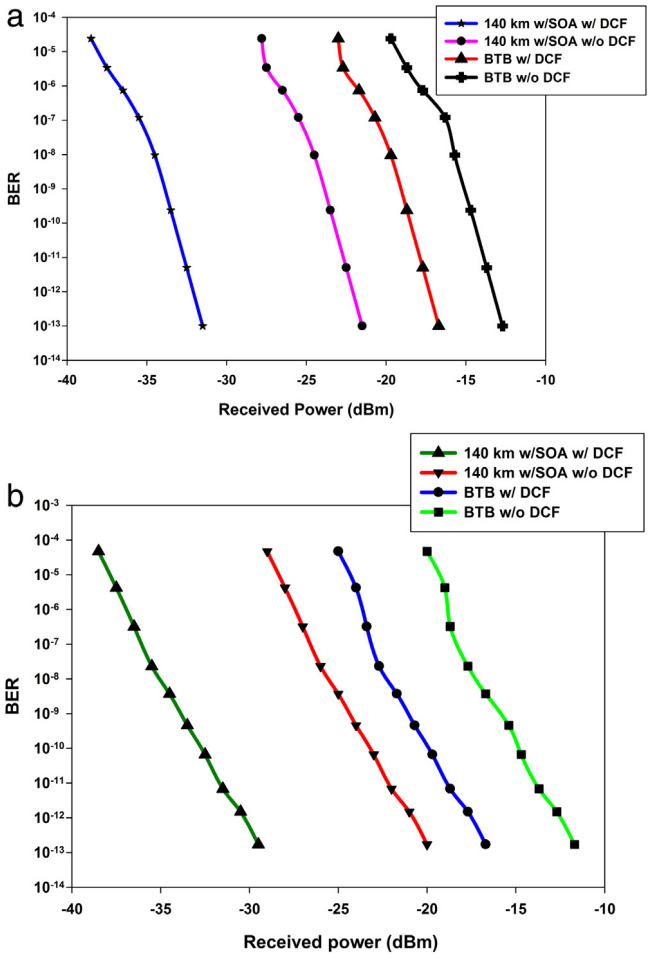

Fig. 5. BER performance as a function of received power for (a) downstream signal at 1597.74 nm and (b) upstream signal at 1544.11 nm.

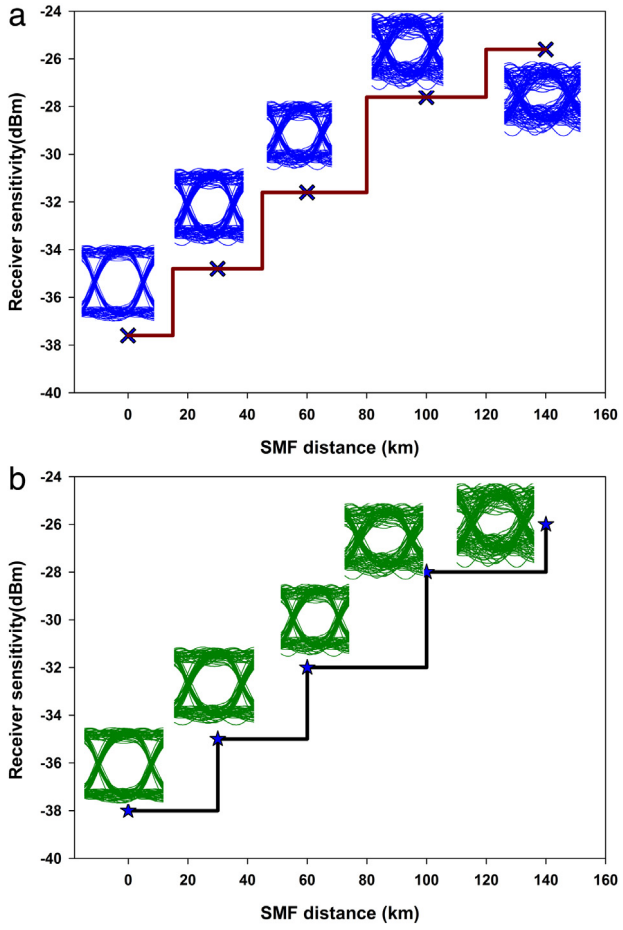

Fig. 6. Receiver sensitivity as a function of SMF distances (a) downstream signal at 1597.74 nm and (b) upstream signal at 1544.11 nm.

For the upstream direction, four working DMLs are used as the upstream transmitters with a tunable range of 3.2 nm. The DMLs are thermally tuned to four wavelengths separated by 0.8 nm which are set at 1541.71,1542.51,1543.31 and 1544.11 nm, where each wavelength has an output power of 20 dBm. After combining and passing through 140 km SMF, the upstream signals are first injected into an EDFA with 20 dB gain and 3.5 dB NF for amplification before being sent to the DCF. Further, an SOA with 18 dB gain and 6 dB NF follows after to improve the receiver sensitivity. Both NF and gain parameters in optical amplifiers can play a significant role in degradation and improvement of the system link performance. The values of NF and gain are chosen to be suitable for the circumstance of the design and in principle, any NF link can be overcome with a sufficiently high gain. In other words, increasing the gain while reducing the NF is possible to a limit that makes the approach of amplification more feasible, where the NF is a critical parameter in the system link amplifier application and should be as low as possible since it determines the lowest achievable sensitivity value. Hence, the interaction between both gain and NF need to be manageable and meet values that have interests in both fundamental and practical demands [27].

Finally, a WDM DEMUX is directed to four upstream channels. The DEMUX also plays a role to suppress the ASE noise from a SOA since it effectively serves as a BPF. An APD at RX is assigned for each channel to directly detect the desired upstream channel for upstream performance evaluation. Finally, with respect to the cost of the ONU structure, we recommend to place a DCF at the OLT to reduce the cost of ONU since it is very important to take the cost effectiveness of ONU into consideration for TWDM-PON architecture. Furthermore, the SOA at ONU will not be too highly attributed for the benefit of the design. As a whole, better performance induces higher cost, but our goal is to maximize the performance to cost ratio for TWDM-PON applications. The spectrum of downstream and upstream wavelengths is demonstrated in inset (i) and (ii) of Fig. 7.

3.2. Result

We evaluate a symmetric 40 Gb/s TWDM-PON system performance for four channels for both downstream and upstream transmission utilizing the DCF as an alternative to improve the power budget of TWDM-PON. Fig. 8(a) and (b) show the BER curves for downstream and upstream signals via DMLs sources against the received optical power after 140 km SMF transmission of the four downstream and upstream signals, respectively. The obtained power penalty between the downstream signals after transmission is less than 1.5 dB at BER of 10^{-5} with receiver sensitivity of -36.6 dBm. However, the upstream signals after transmission demonstrate more than 2.4 dB power penalty at BER of 10^{-5} where the receiver sensitivity is -36.8 dBm.

For both directions, the results show a significant variation of signal qualities which lead to significant power penalties; this is mainly influenced by the wavelength bands where the wavelengths have different conditions. Dispersion is induced from the fiber transmission in addition to there being no specific technique for the DMLs chirps other than controlling the most critical parameters that play a significant role to improve the transmission performance with the help of DCF technique. The downstream and upstream wavelengths are in different wavelength

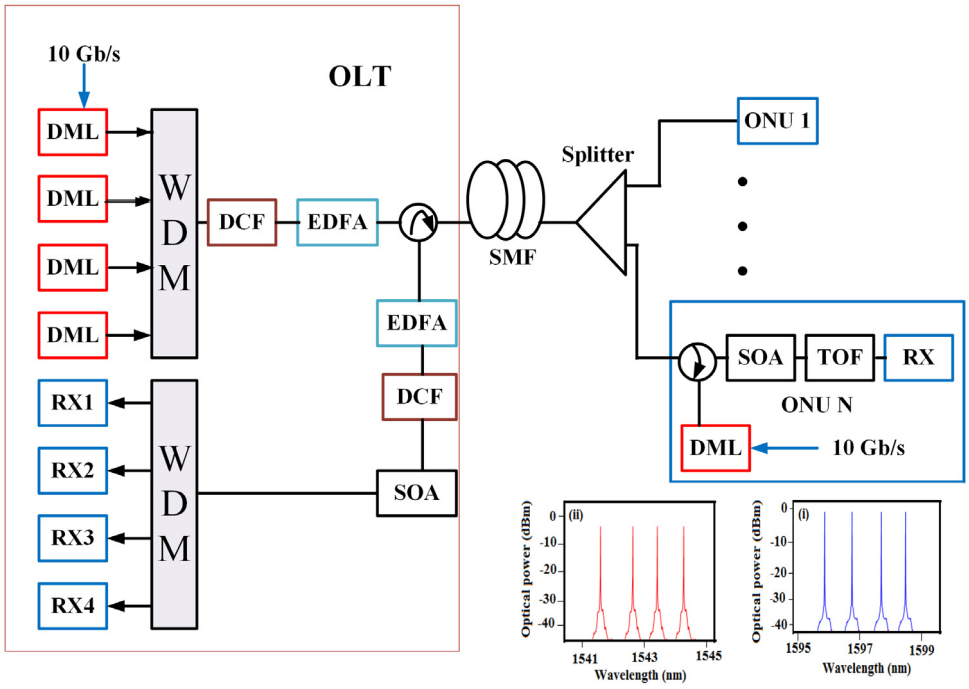

Fig. 7. 40 Gb/s TWDM-PON system with dispersion compensation, the inset (i) the spectra of the downstream channels, (ii) the spectra of the upstream channels.

Table 3
Power budget evaluation TWDM-PON system.

	Downstream		Upstream	
	140 kmw/DCF(1 channel)	140 km w/DCF(4 channel)	140 kmw/DCF(1 channel)	140 km w/DCF(4 channel)
Transmitted power (dBm)	20	20	20	20
Received sensitivity	−38.1	−36.6	−38.5	−36.8
Fiber loss (dB)	28	28	28	28
Splitting loss (dB)	27	27	27	27
Total loss (dB)	55	55	55	55
Power budget (dB)	58.1	56.6	58.5	56.8

bands with large wavelength difference between both directions. Hence, the effect of cross gain modulation (XGM), cross phase modulation (XPM) and four wave mixing (FWM) between the downstream and upstream signals are minimal. This work exhibited a significant improvement to the previous works [5,19] that deploy DI or filtering as their mechanism of chirp mitigation. As a result of high DML tolerance to high power as reported in [28], more users can be supported due to the increase in power budget. Using the SOA as amplifier and directly boosting the signal induces a strong pattern effect, hence the eye diagram the BER cannot be obtained. Therefore, the power injected to the SOA amplifier should be small for boosting linear amplification as reported in [18].

3.2.1. Power budget evaluation

The concept of power budget is determined by the transmitted power and the receiver sensitivity. The transmitted power is 20 dBm for downstream and upstream single channel respectively leading to power budgets of 58.1 for the downstream and 58.5 dB for the upstream direction, respectively. The receiver sensitivity for four channels is -36.6 and -36.8 dBm for downstream and upstream directions respectively, taking into consideration that the transmitted power is 20 dBm for both directions. Therefore, this results in power budgets of 56.5 and 56.8 dB, respectively, for the downstream and upstream directions among the transmitted four channels. Finally, according to the sensitivity of the received signal and the output power of the laser source, the proposed scheme of 40 Gb/s TWDM-PON architecture supports up to 512 splits over 140 km SMF transmission distance estimated power budget of 56.6 dB. The detailed downstream and upstream power budgets are shown in Table 3, where the loss of all other passive components has already been neglected. It should be noted that the system power budget of 56.6 dB is observed at the downstream direction where the launched power is limited by the cross phase modulation effect between different channels.

We provide a comparative view of the power budget capabilities of TWDM-PON system. In existing research of power budget on TWDM-PON system, the main objective is to minimize the cost consumption of the system while improving the services to the remote places. Even though existing studies on TWDM-PON system, have reported acceptable constrained long reach, these studies have not considered an improved power budget to remote places on TWDM-PON system environment. We compare the power budget performance of our proposed scheme against other published work of TWDM-PON system, as shown in Table 4. Since we do not have a TWDM-PON system testbed yet in our lab, we compare our proposed scheme with experimental schemes existing in the literature. However, the reported power budget can achieve the similar budget with the experiment TWDM-PON system, so we believe the power budget in simulations procedure is comparable in this view.

A range of power budget between 31 to 53 dB is achieved that correspond to different maximum supported users, transmission distance and splitting ratio. The previous schemes used delay interferometer (DI), specially designed tunable optical filter (TOF), Duo-binary modulation format and pulse amplitude modulation (PAM-4) modulation format as dispersion compensators to mitigate the dispersion of DML and SMF on TWDM-PON for the different transmission distance. As shown in Table 4, the previous schemes power budgets are 53, 51, 43.2, 39 and 38 dB which support 100, 40, 100, 25, and 50 km fiber transmission

Table 4
Comparisons of Power budget performance for our proposed TWDM-PON system.

Parameter	Proposed scheme	Scheme in [19]	Scheme in [18]	Scheme in [5]	Scheme in [16]	Scheme in [15]
Transmission distance (km)	140	100	40	100	25	50
Splittingratio	1:512	1:512	1:2000	1:64	1:1024	1:256
Powerbudget (dB)	56.6	53	51	43.2	39	38
Key technique	DCF	DI	SOA	DI	Special designed TOF	DI

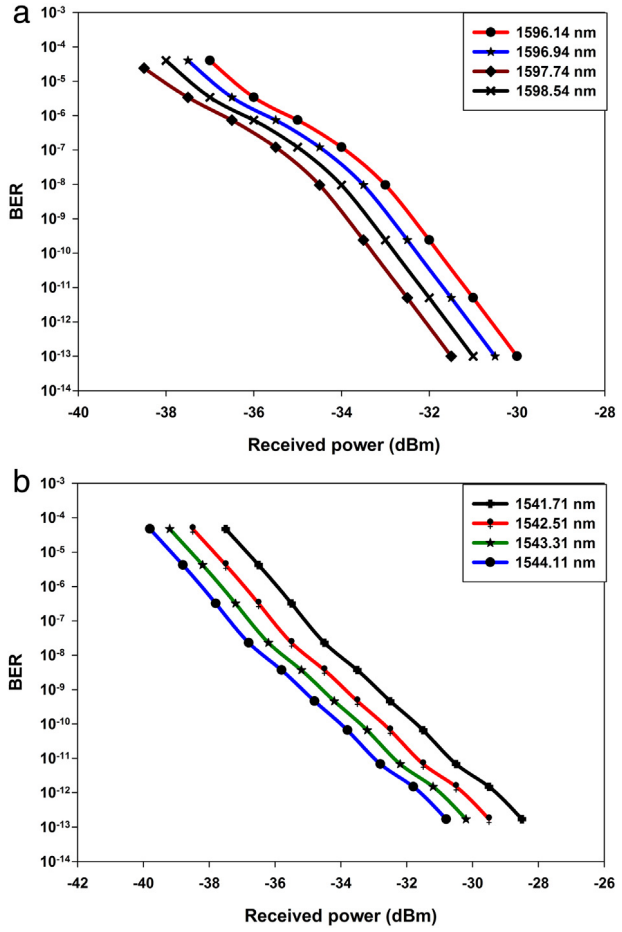

Fig. 8. BER as a function of received power for (a) downstream signals and (b) upstream signals.

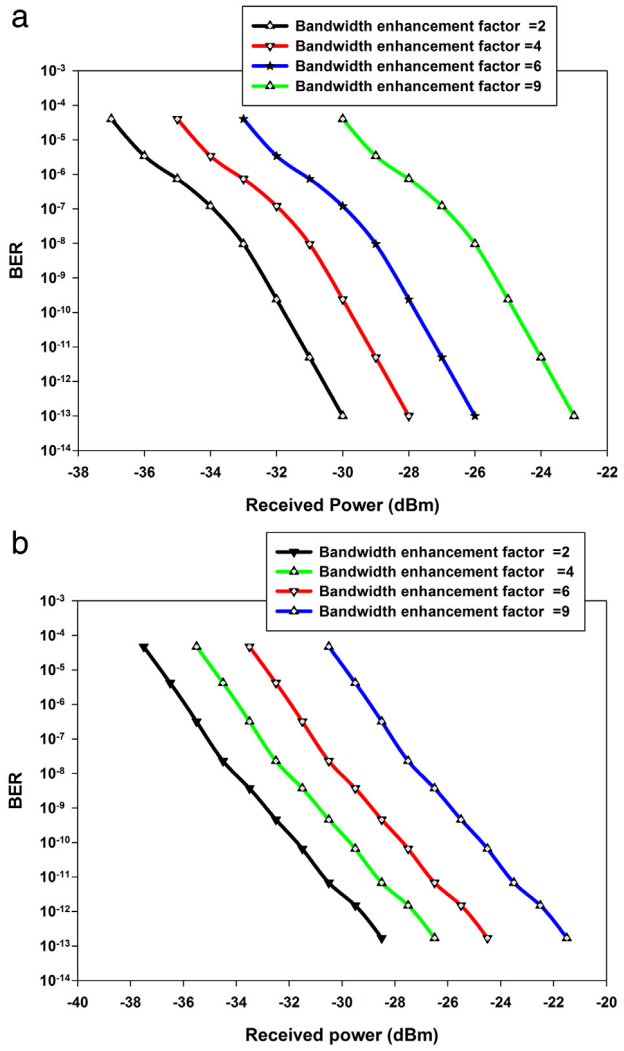

Fig. 9. BER performance as a function of received power under different α values.

distance and 1:512,1:2000, 1:64, 1:1024, and 1:256 splits, respectively. Compared to the above results, the power budget of our scheme has the highest value that could support up to 512 splits over 140 km fiber distance.

4. Feasibility investigation

4.1. Bandwidth enhancement factor (α) feasibility

We investigate the influence of random values of bandwidth enhancement factor α of DML on TWDM-PON system performance for both downstream and upstream direction. Fig. 9 illustrates different BER performance of TWDM-PON system as a function of the received power under different α values. As clearly presented in both Fig. 9 (a) and (b), the performance improves with the decrease in the α values. When the α decreases, the DML can transmit high data rate at both OLTs and ONUs, thereby increasing bandwidth spectral of DML.

When α increases, the DML cannot transmit high data rate at both OLTs and ONUs due to the effect of frequency chirp; thus, decreasing the bandwidth spectral as a small α values helps to prevent the effect of the inter-symbol interferences in DML transmission characterization. For α value of 2, the receiver sensitivity is -36.4 dBm at BER of 10^{-5} for downstream link while the receiver sensitivity is -36 dBm at BER of 10^{-6} for upstream link as shown in Fig. 9(a) and (b), respectively. For α of 9, the receiver sensitivity is -28.6 dBm at BER of 10^{-5} for downstream link while the receiver sensitivity is -27.8 dBm at BER of 10^{-6} for upstream link as shown in Fig. 9(a) and (b), respectively. Based on the outcome of this investigation, it is important to note that the α value plays an important role in the aspect of DML frequency chirp effect in this work. However, our results indicate that the α of the DML is in acceptable range to support the quality of services requirements of practical access networks.

4.2. Power budget with dispersion feasibility

While the main goal of this work is to improve the power budget of the TWDM-PON system, this investigation aims to consider the length

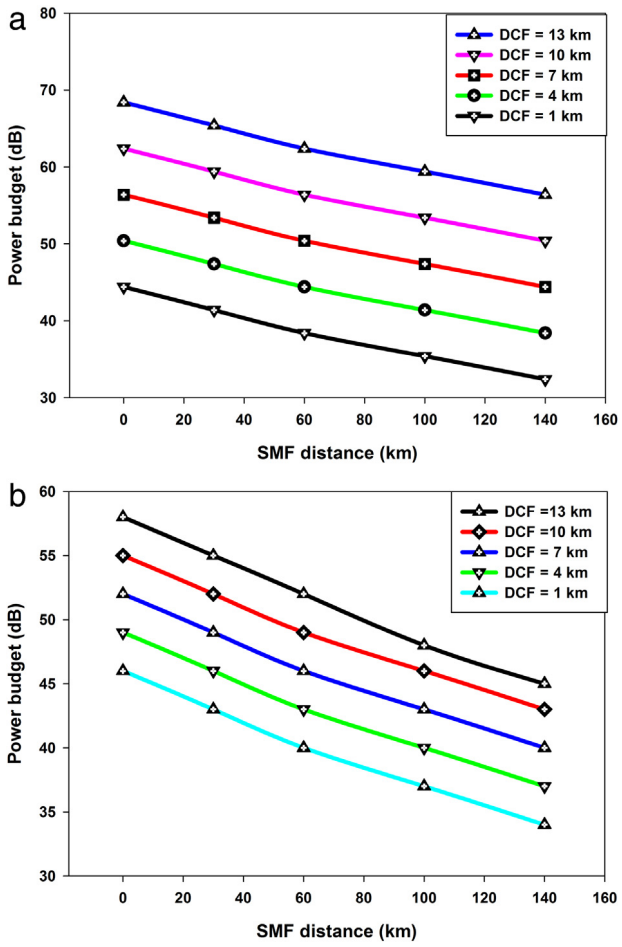

Fig. 10. Power budget as a function of SMF distance with different DCF lengths for (a) downstream link at BER of 10^{-5} and (b) downstream link at BER of 10^{-6}.

of the DCF to get the whole system power budget. Fig. 10(a) and (b) illustrate the whole system power budget achieved as a function of SMF distance under different DCF lengths for both downstream and upstream links, respectively.

It is clearly observed that, without DCF, an increasing fiber length brings in power budget reduction, resulting from the residual dispersion induced system degradation. This effect worsens the power budget and subsequently reduces the long reach that system can support. For a specific fiber length, a suitable DCF length is required, thus a large power budget is observed. In addition, it can be seen in Fig. 10(a) and (b), for the DCF length of 1 km, the power budget of both downstream and upstream links of ~32.2 dB can be obtained for the fiber length of 140 km. When the DCF length increases to 4 km, we achieve power budget of ~38.2 dB over 140 km SMF. As the DCF length increases to 7 , 10 and 13 km, the power budgets of ~ 44, 50, and 56 dB are achieved over 140 km SMF where the accommodated users is fixed in this investigation, which is 512 users. Hence, from above analysis, it can be seen that the system power budget is adjustable when different DCF is adopted as the DCF with SMF distance length is strongly correlated to the whole system power budget.

5. Conclusion

We propose to use a DCF in OLT to improve the loss budget of 40 Gb/s TWDM-PON system. The distortion resulting from the DML is minimized by output optical power and enhancement bandwidth factor based on signal rate equations. 56.6 dB power budget is achieved with the ability to support 140 km fiber transmission and more than 512 users.

Our simulation results demonstrate a sufficient dispersion compensation for DML-based TWDM-PON transmission system. While results are not absolute due to variations that can occur in practical implementation, our analysis demonstrates the feasibility of using DCF to improve the power budget of 40 Gb/s TWDM-PON links.

Acknowledgments

The work described in this paper was carried out with the support by a research management center (RMC) of University Technology Malaysia (UTM). The authors acknowledge the Ministry of Higher Education Malaysia (MOHE) and the administration of UTM for the project financial support through the cost center number Q. J130000.2523.18H19.

References

[1] D. Nesset, NG-PON2 technology and standards, J. Lightw. Technol. 31 (4) (2013) 587–593.
[2] N. Cheng, Flexible TWDM-PON with WDM overlay for converged services, Opt. Fiber Technol., Mater. Devices Syst. 26 (2015) (2015) 21–30.
[3] Y. Luo, H. Roberts, K. Grobe, M. Valvo, D. Nesset, K. Asaka, H. Rohde, J. Smith, J.S. Wey, F. Effenberger, Physical layer aspects of NG-PON2 standards—Part 2: System design and technology feasibility, J. Opt. Commun. Netw. 8 (1) (2015) 43–52.
[4] P.P. Iannone, A.H. Gnauck, D.T.V. Veen, V.E. Houtsma, Increasing TDM rates for access systems beyond NG-PON2, J. Lightw. Technol. 34 (6) (2016) 1545–1550.
[5] M. Bi, S. Xiao, L. Yi, H. He, J. Li, X. Yang, W. Hu, Power budget improvement of symmetric 40-Gb/s DML-based TWDM-PON system, Opt. Express 22 (6) (2013) 6925–6933.
[6] I. Tomkos, D. Chowdhury, J. Conradi, D. Culverhouse, K. Ennser, C. Giroux, B. Hallock, T. Kennedy, A. Kruse, S. Kumar, N. Lascar, I. Roudas, M. Sharma, R.S. Vodhanel, C.-C. Wang, Demonstration of negative dispersion fibers for DWDM metropolitan area networks, IEEE J. Sel. Top. Quantum Electron. 7 (3) (2001) 439–460.
[7] I. Tomkos, B. Hallock, I. Roudas, R. Hesse, A. Boskovic, J. Nakano, R. Vodhanel, 10-Gb/stransmission of, 10-Gb/s transmission of 155- m directly modu-lated signal over 100 km of negative dispersion fiber, IEEE Photon.Technol. Lett. 7 (13) (2001) 735–737.
[8] P.J. Winzer, F. Fidler, M.J. Matthews, L.E. Nelson, H.J. Thiele, J.H. Sinsky, S. Chandrasekhar, M. Winter, D. Castagnozzi, L.W. Stulz, L.L. Buhl, 10-Gb/s Upgrade of Bidirectional CWDM Systems Using Electronic Equalization and FEC, J. Lightw. Technol. 31 (4) (2005) 203–210.
[9] C. Sun, S.H. Bae, H. Kim, Transmission of 28-Gb/s duobinary and PAM-4 signals using DML for optical access network, IEEE Photon.Technol. Lett. 13 (7) (2017) 130–133.
[10] N. Cheng, M. Zhou, F.J. Effenberger, 10 Gbit/s delay modulation using a directly modulated DFB laser for a TWDM-PON with converged services, J. OPT. COMMUN. NETW. 7 (1) (2015) A87– A96.
[11] N. Cheng, X. Yan, N. Chand, F. Effenberger, 10 Gb/s Upstream Transmission in TWDM-PON Using Duobinary and PAM-4 Modulations with Directly Modulated Tunable DBR Laser, presented at the Asia Commun. Photon. Conf. Exhib. Beijing, China, 2013, Paper ATh3E4.
[12] Z. Li, L. Yi, M. Bi, J. Li, H. He, X. Yang, W. Hu, Experimental demonstration of a symmetric 40-Gb/s TWDM-PON, presented at the Opt. Fiber. Commun. Conf. Anaheim, CA, USA, 2013, Paper. NTh4F3.
[13] Z. Li, L. Yi, X. Wang, W. Hu, 28 Gb/s duobinary signal transmission over 40 km based on 10 GHz DML and PIN for 100 Gb/s PON, Opt. Express 23 (16) (2015) 20249–20256.
[14] Z. Li, L. Yi, H. Ji, W. Hu, 100-Gb/s based on 10 G optical devices, Opt. Express 24 (12) (2016) 12941–12948.
[15] Y. Luo, X. Zhou, F. Effenberger, X. Yan, G. Peng, Y. Qian, Y. Ma, Time and wavelength-division multiplexed passive optical network (TWDM-PON) for next-generation PON stage 2 (NG-PON2), J Lightw. Technol. 31 (4) (2013) 587–593.
[16] M. Bi, S. Xiao, H. He, L. Yi, Z. Li, J. Li, X. Yang, W. Hu, Simultaneous DPSK demodulation and chirp management using delay interferometer in symmetric 40-Gb/s capability TWDM-PON system, Opt. Express 21 (14) (2013) 16528–16535.
[17] L. Yi, Z. Li, M. Bi, W. Wei, W. Hu, Symmetric 40-Gb/s TWDM-PON with 39-dB power budget, IEEE Photon. Technol. Lett. 25 (7) (2013) 644–647.
[18] Z. Li, L. Yi, W. Hu, Symmetric 40-Gb/s TWDM-PON with 51-dB loss budget by using a single SOA as preamplifier, booster and format converter in ONU, Opt. Express 22 (22) (2014) 24398–24404.
[19] Z. Li, L. Yi, W. Wei, M. Bi, H. He, S. Xiao, W. Hu, Symmetric 40-Gb/s, Symmetric 40-Gb/s 100-km passive reach TWDM-PON with 53-dB loss budget, J. Lightw. Technol. 23 (21) (2014) 3991–3998.

[20] J. Wang, K. Petermann, Small signal analysis for dispersive optical fiber communication svstems, J. Lightw. Technol. 10 (1) (1992) 96–100.
[21] A.S. Karar, J.C. Cartledge, J. Harley, K. Roberts, Electronic pre-compensation for a 107-Gb/s system employing a directly modulated laser, J. Lightw. Technol. 29 (13) (2011) 2069–2076.
[22] T.L. Koch, J.E. Bowers, Nature of wavelength chirping in directly modulated semiconductor lasers, Electron. Lett. 2 0(25) (1984) 1038–1040.
[23] C. Henry, Theory of the linewidth of semiconductor lasers, IEEE Journal of Quantum Electronics 18 (2) (1982) 259–264.
[24] K. Sato, S. Kuwahara, Y. Miyamoto, Chirp characteristics of 40-Gb/s directly modulated distributed-feedback laser diodes, J. Lightw. Technol. 29 (13) (2005) 3790–3797.
[25] L. Bjerkan, A. Rgyset, L. Hafskjaer, D. Myhre, Measurement of laser parameters for simulation of high-speed fiber optic systems, J. Lightw. Technol. 14 (5) (1996) 2069–2076.
[26] D. Mitić, A. Lebl, Ž. Markov, Calculating the required number of bits in the function of confidence level and error probability estimation, Serbian J. Electr. Eng. 9 (3) (2012) 361–375.
[27] D.R. Zimmerman, L.H. Spiekman, Amplifiers for the masses: EDFA, EDWA, and SOA amplets for metro and access applications, J. Lightw. Technol. 22 (1) (2004) 63–70.
[28] Z. Li, L. Yi, W. Hu, Comparison of downstream transmitters for high loss budget of long-reach 10G-PON, presented at the Opt. Fiber. Commun. Conf. San Francisco, CA, USA, 2014, Paper Tu2C4.